In 2023 IEEE/AIAA 42nd Digital Avionics Systems Conference (DASC), 1-5 October 2023, Barcelona, Spain
DOI: 10.1109/DASC58513.2023.10311236

Conflict Probability Based Strategic Conflict Resolution for UAS Traffic Management

Yiwen Tang, Yan Xu, Gokhan Inalhan
School of Aerospace, Transport and Manufacturing
Cranfield University
Bedford, United Kingdom
{yiwen.tang, yanxu, inalhan}@cranfield.ac.uk

***Abstract*—In this paper, we present a strategic conflict resolution method based on the conflict probability estimation, in the context of Unmanned Aircraft System (UAS) Traffic Management. We first elaborate a classic approach for flight trajectory generation in a designated realistic airspace environment, which is then smoothed by B-spline algorithm to achieve higher realism. The trajectories are extended to 4-dimensional Operational Volumes (OV) following the current UTM development visions. This forms the basis for performing a coarse conflict screening process, as the initial part for conflict detection, primarily based on identifying any OVs overlapping in temporal and spatial. Next, we look into the captured OVs and apply a well-studied conflict probability estimation approach, which contributes to a refined and more accurate conflict detection outcome. To resolve the potential conflicts, we propose two models including First-Come, First-Served (FCFS) and optimisation, both embedded with the probability-based conflict detection. In the FCFS approach, flights are delayed in the order of their submission, while the optimisation model aims at cherry-picking flights to seek the optimal solution. Numerical experiments with various case studies are performed to assess the effects with and without such probability concern, as well as different implementation strategies in real world. Results suggest that, allowing OVs' overlapping to some extent does not necessarily incur conflict over an acceptable probability, whereas the efficiency of airspace use could be improved.**

***Index Terms*—Strategic conflict resolution, UAS traffic management, U-space, conflict probability, operational volume**

I. Introduction

With the increasing demand for unmanned aerial systems (UAS) applications, the establishment of dedicated UAS traffic management (UTM) systems has become an urgent need for achieving the seamless, safe, and equitable integration of UAS into the airspace. Currently, the exploration of UTM concepts is progressing rapidly. Organizations such as the National Aeronautics and Space Administration (NASA) and the Federal Aviation Administration (FAA) have introduced fundamental principles and potential scenarios for very low level (VLL) airspace operations [1] [2]. Additionally, Europe has developed a vision for future operations through the concept of operations (ConOps), which aims to enable more advanced and efficient operations [3] [4].

UTM defines a hierarchical conflict management approach that ensures safety up to a designated level by having its layers working together, which consists of strategic deconfliction, tactical separation provision, and collision avoidance. Concretely, strategic conflict resolution (SCR) service is referred to as the initiatives aiming to reduce the need from downstream tactical operation. The service typically occur at the pre-flight phase, which involves conflict detection and then resolution. This requires operators sharing the flight plans with relevant parties and reducing any potential loss of separation by planning routes that are unlikely to cause interactions with other airspace users.

As a commonly used method for this service these days, the U-space Service Provider (USSP) checks for any intersections in space and time between newly submitted flights and previous ones based on the First-Come, First-Served (FCFS) principle. Necessary airspace volumes are then reserved to cover the entire operation once the conflict is resolved. According to the U-space concept of operation, the intersection of two operation plans may be interpreted in different ways during strategic conflict prediction process [3]. Specifically, usually the flight trajectory is represented by a series of waypoints in 4 dimension. To include operational uncertainties into the flight, a certain range will be extended outward taking the trajectory as the center line. The first approach involves representing each point of the trajectory as a 4-dimensional volume, providing a pre-definded buffer size for each point, such as explored in [5]. Alternatively, the operation can be represented by a 4-dimensional space along the trajectory, defining the potential range in which the UAS will operate within for a certain probability (such as 95%), with an example illustrated in [6] applying data-driven approach. Both approaches ensure that the uncertainties associated with UAS operations are considered, while the second one could further include conflict probability estimation.

During the initial stages of developing this service, previous work have explored various perspectives to enhance its functionality and performance. These includes efforts to improve efficiency through airspace management [7], consider the trade-off between fairness and efficiency [8], and investigate the problem under decentralised structure [9]. Among them, most of the conflict detection is based on the volume-based overlap. For example, 4D protection bubbles around the UAS were introduced to ensure the separation between vehicles in [10], where conflict risk was analysed and categorised to indicate the collision severity. The suitability of operational volumes for strategic deconfliction was evaluated in [11] to

provide guidance for risk reduction. Optimisation approach was incorporated to the strategic conflict resolution service to solve the intersection detected by iteratively checking the availability of the shared airspace volumes in previous work [5]. However, when the traffic density increases, preventing any overlap between buffer volumes may be inefficient for the overall system performance, resulting to excessive airspace occupancy from both time and space perspective and thus inflexible airspace utilisation.

To tackle this issue, a careful conflict detection will be needed for such a service to incorporate conflict probability estimation. These would potentially allow for the acceptance of partial, insignificant intersection when the estimated collision probability falls below an acceptable safety threshold. According to the guiding principles published by [12], the service should allow for overlapping operational volume (OV), given that other conflict mitigations are in place. The concept of OV is employed to represent the intended operation intent and encompass the buffer airspace that should cover the operating range of the UAS in case of uncertainty, serving as a primary subject for conflict detection. As indicated in ASTM standard [13], the 4D OV should contain its respective flight 95% of the time to meet the balance between safety and efficiency. Prior study also investigated the relationship between the OV buffer size and the relative risk [11]. Then it will be reasonable to assume that not all flight segments with intersected OV are likely to result in conflicts, such as those segments only intersected at their margins.

A number of studies have explored methods for estimating conflict probability, which can be generally categorised to analytical and simulation approaches. In the analytical approach, ICAO has adopted the Reich collision risk model in [14] to estimate the collision probability for manned aviation during the en-route phase. Considering the characteristics of the UAS, this study [15] established three types of collisions zone for UAS and delved into the respective collision probability calculation algorithms. In the simulation approach, Monte Carlo simulations have been widely employed to estimate the probability of conflicts in traffic encounters. As a key input parameter of such simulations, a series of simulations have been performed based on probability density functions to project the position uncertainties of a aircraft [16]. While these studies mainly focus on the tactical phase, the underlying principles of probability estimation are similar to those that could be leveraged in the strategic phase. A typical use case can be found in the BUBBLES project which employed the GAS model [17] to obtain approximate conflict rate results [18]. It further applied machine learning techniques [19] to compute the suitable separation minima that meets the target safety level in strategic and tactical mitigations.

This study proposes a conflict probability-based approach for the strategic conflict resolution service. The main idea is to estimate the likelihood of conflict between intersected operational volumes, thus detecting flights only with unacceptable conflict possibilities, and then mitigate the conflicts accordingly. We first introduce flight planning in an airspace

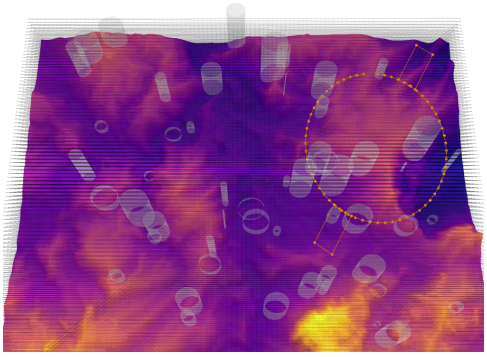

Fig. 1: Airspace environment divided into discrete volumes.

environment built on real-world data, where a B-spline method is utilised to smooth the trajectory. The trajectory is then extended leveraging the concept of Operational (Intent) Volume (OVs) to accommodate flight-associated uncertainties. The coarse conflict screening is then carried out to initially capture the OVs only with intersections meaning potential conflicts, whose probability can be estimated using a well studied approach. This is then fully integrated with a FCFS approach and an optimisation approach respectively to resolve the conflict by means of delay. To evaluate the effects of the approaches, numerical experiments have been conducted in three case studies following different implementation strategies, with results compared between resolution with and without considering conflict probability.

II. Conflict Detection

This section first introduces briefly how the flight trajectories are produced and then extended to OVs to accommodate uncertainties, which are the key input to the conflict detection. Next, a coarse conflict screening process is elaborated and followed by delving deep into a pair of identified OVs to estimate the accurate conflict probability.

A. 3D airspace modelling

In this study, we begin by constructing a fundamental 3-dimensional (3D) airspace environment model. The airspace is divided into discrete volumes, each possessing the same dimensions, as illustrated in Fig. 1. The central point of each

Fig. 2: Altitude Angel drone safety map.

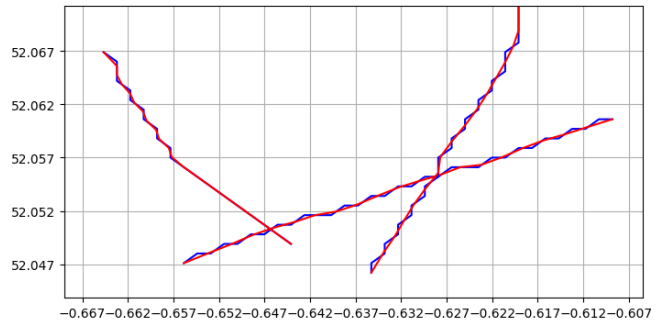

Fig. 3: Smoothed flight trajectories using B-spline curve (Blue lines: original trajectories; Red lines: smoothed trajectories).

airspace volume is denoted by evenly distributed black dots in the figure. To facilitate trajectory generation, each volume is connected to its adjacent volumes in ten directions (eight horizontally and two vertically), except for those that intersect airspace constraints or reside on the boundary.

To ensure realism, real-world environmental data is integrated, encompassing terrain features, ground obstacles, major road networks, and restricted airspace. The figure illustrates the altitude variation of the terrain within the airspace. The colour scheme indicates altitude levels, with lighter shades representing higher altitudes and darker shades representing lower altitudes. The restricted airspace surrounding the airport is delineated by the orange lines. The real-world aeronautical and ground hazards data utilised in this study is sourced from Altitude Angel's Drone Safety Map [20], as illustrated in Fig. 2. Additionally, geo-fence is introduced as an airspace constraint to regulate drone access. This geo-fence is represented by the grey cylinder in the figure and imposes an upper altitude limit, with the lower bound being the ground level. To mirror actual operational conditions, all factors within the airspace environment are taken into account during the subsequent trajectory generation process.

B. Flight trajectory generation

Following our previous work [21], only linear trajectory such as for delivery missions is considered in this study. It follows the vertical take-off and landing (VTOL) characteristic to mimic the UAS moving pattern in real operations. The classic A* algorithm is applied to search for the shortest path (bypassing geo-fences and obstacles). Specifically, once the UAS reached the top of climb altitude, it will enter the cruise phase, during which the A* algorithm is applied to search the shortest path from the adjacent volumes in 8 horizontal directions as mentioned above, using the UAS as the centre point, and then descent when it reaches the top of descent point. On top of the generated path, timestamps are attached from the take-off time at its first point and iterated over each trajectory segment at a given speed until the last point for landing time.

The trajectory generated by A* algorithm on the grid may contain zigzag-shaped flight segments. To improve the realism,

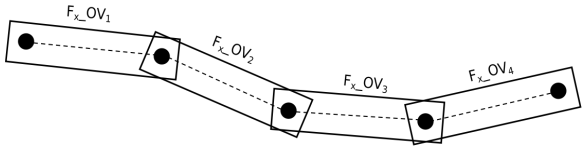

(a) Schematic of Operational (Intent) Volumes

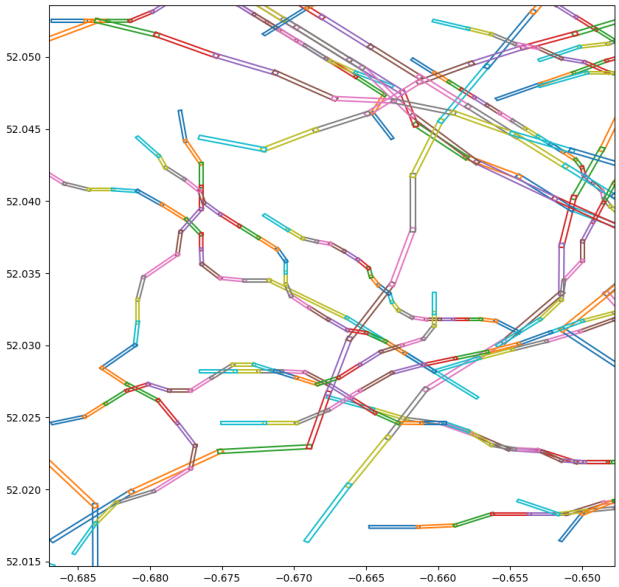

(b) Operational Volumes centred on generated trajectories

Fig. 4: Flight trajectories extended to Operational Volumes.

we employ a B-spline method, a widely used technique for path smoothing. Compared to other trajectory smoothing methods, B-spline curve is independent from the number of control points. The basic functions have local control of the curve, which allows modifications of any path segment, without affecting the neighboring segments, or changing the shape of the entire curve [22]. As shown in Fig. 3, the blue lines represent the original zigzag trajectories generated by A* algorithm, while the red ones are the smoothed trajectories obtained through the B-spline method. The zigzag segments have been effectively smoothed out, resulting in a more reasonable trajectory shape in reality.

C. Operational volume extension

Safety protection zone around each UAS operation is needed as the current UAS techniques may involve significant uncertainties that could lead to undesirable consequences. In our previous research, expanded uncertainty buffers volumes are attached to each airspace volume that is planned to be traversed to provide protective space in response to potential uncertainties. However, the expanded uncertainty buffer comes with drawbacks, including introduced computational complexity and limitation on the application scope. To avoid the above issue while ensuring safety, we apply the OV concept in this study. This also allows to transform the conflict detection

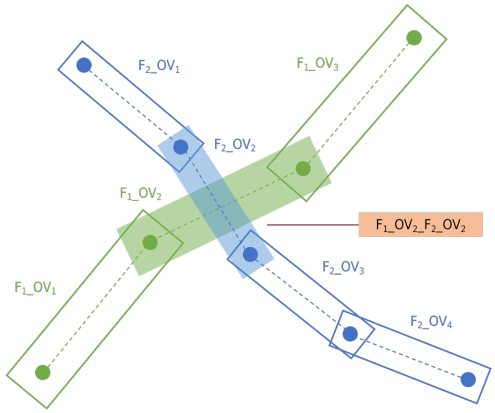

(a) Intersected OVs in space

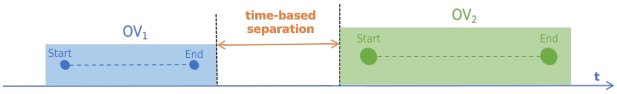

(b) Intersected OVs in time

Fig. 5: Coarse conflict screening based on both OVs' intersection and associated time windows.

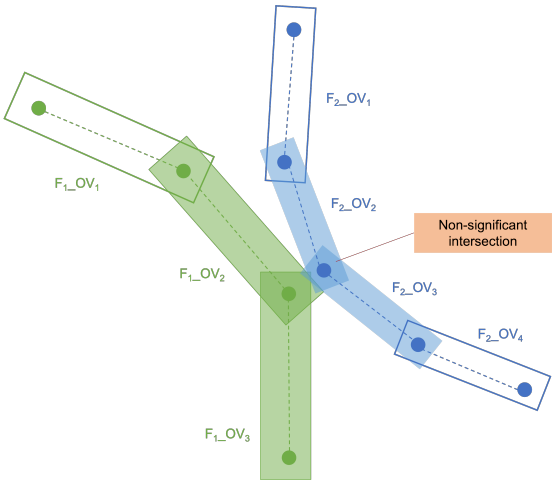

Fig. 6: Example of a non-significant intersection.

subject from the entire flight trajectory to each individual OV across the flight.

Each flight trajectory consists of several flight segments. The OV is then built based on each flight segment and expands outward to a certain size to provide a sufficient safety uncertainty buffer, as illustrated in Fig. 4a. It is expected to be a 4D cuboid defining the horizontal and vertical bounds of airspace and the corresponding volume start and end times (which correspond to the earliest entry time and the latest exit time, respectively) to which the flight is intended to conform [13]. The size of the OV in this study draws inspiration from the concept of Performance Based Navigation (PBN) [23], which is a concept used in the field of ATM to define a specific range where an aircraft is expected to operate with a high probability in normal situations. The lateral distance from the boundary of the OV to the centerline of the trajectory will be influenced by the total system error (TSE) of the UAS, which largely depends on flight performance. Previous studies [24] [25] have explored TSE for some specific UAS types. As the estimation of the TSE may require experimental and kinetics analysis to specific UAS, this issue is beyond the discussion of this paper. The generated OV is illustrated in Fig. 4b, represented by different colours, indicating different flight segments of a flight. The size and length of each OV may differ, reflecting the specific performance of each UAS. The intersecting OVs, as highlighted in in Fig. 4b, indicate potential conflicts, which is the starting point of conflict detection to be discussed below.

D. Coarse conflict screening

Conflict detection can be divided into a number of steps, from the preliminary screening of possible conflict to the final examinations. Based on the OV concept introduced in Sec. II-C, conflicted flight pairs can be found by coarsely screening the intersected OVs. For any spatial overlapped OVs, it indicates potential conflict. These OV pairs will be captured for further conflict examination in next steps. As shown in Fig. 5a, flight F_1 is intersected with flight F_2 at their second OVs (marked as OV_2), where the intersection is denoted as $F_1\_OV_2\_F_2\_OV_2$. Based on this, when examining potential conflicting flights, we begin with the evaluation directly from the intersecting OVs rather than analysing the entire set of OVs, which will largely reduce the computational complexity.

Next, regarding the OVs that are initially captured, we further check the OVs by time-based separation minima. The time difference between the arrival time of one OV and the start time of another will be compared with the specified time-based separation threshold, as illustrated in Fig. 5b. If the difference is greater than the threshold, it means that one flight enters an airspace volume until another flight leave, therefore no conflict will be considered between the OVs. Otherwise, it indicates a potential conflict may exist and the pair of OVs will be captured for further examination. By incorporating the time-based separation, we can also refine the selection of OV pairs and focus on those with a higher likelihood of actual conflicts.

The conflict detection for strategic phase usually ends at this step. However, such OV pairs, having both time and space overlapped, may only incur a negligible conflict probability, which is the main argument of this study, namely, tolerating some intersected OVs with low conflict probability could contribute to improved use of the airspace. Thus, a reliable method is needed to well estimate the conflict probability for those intersected OV pairs.

E. Conflict probability estimation

After the corse screening process, it is possible to initially identify if two flights are in conflict. However, this coarsely filtering method may result in including non-significant overlaps as conflicts, leading to unnecessary delays during the subsequent conflict resolution process. In some cases, two

OVs may not have obvious intersections in spatial perspective, such as when their protection buffer zones are overlapped. As illustrated in Fig. 6, OV $F_2\_OV_2$, OV $F_1\_OV_2$, OV $F_1\_OV_3$ and OV $F_2\_OV_3$ are slightly overlapped at their margins without approaching to the trajectories. In this scenario, to decide whether the two flights are conflicted, we can then estimate the conflict probability between the intersected OVs.

As stated before, current UAS operations may involve significant operational uncertainties, which could make the actual flight to deviate from the planned trajectory. If the position prediction is initiated from the origin point of the trajectory, it is likely to be inaccurate due the accumulated errors. As a result, we focus on individual flight segments, i.e., OVs, as the subject of prediction (recall Sec. II-C). In this study, we assume that the UAS will return to its planned position at the beginning of each OV within the planned entry time window.

We adopt the traditional conflict probability estimation model proposed in [26], where Gaussian distribution is used to represent the positional prediction error. Let $\tilde{q}$ represents the prediction error of the UAS in a heading-aligned two-dimensional coordinates system, then the error can be expressed as $\tilde{q} \sim N_2(0, \Lambda)$, and $\Lambda = \text{diag}(\sigma_a^2, \sigma_c^2)$, with zero mean and with a covariance that has eigenvectors in the along-track σ_a^2 and cross-track σ_c^2 directions.

To transform the heading-aligned coordinates system to the global coordinate system, a rotation matrix R is applied, where

$$R = \begin{bmatrix} \cos\psi & -\sin\psi \\ \sin\psi & \cos\psi \end{bmatrix} \tag{1}$$

where ψ is the UAS heading angle. Then the UAS position error in global coordinate frame can be expressed by $\tilde{p} = R\tilde{q}$, which still follows normal distribution.

Based on the same coordinate system, the covariance of the two UAS can be combined and assigned to one of the UAS, noted as stochastic UAS (marked as S), while the other named as reference UAS (marked as R). As shown in Fig. 7, the combined prediction error is assigned to the stochastic UAS. The circular collision zone is centred on the reference UAS which has no uncertainty.

The position difference between the two UAS is $p = p_S - p_R$, then the prediction error is $\Delta\tilde{p} = \tilde{p_S} - \tilde{p_R}$.

To transform the coordinate system, let p and ρ represent the original and transformed position respectively, then $\rho = Tp$, where T is a transformation matrix. By applying the Cholesky decomposition, the covariance of the transformed position error is converted to $cov(\Delta\tilde{\rho}) = I$. The transformed encounter geometry is shown in Fig. 8, where the combined error ellipse is transformed into the standard form of a unit circle. Then, the probability density function can be decoupled into two identical one-dimensional functions:

$$p(x, y) = p(x)p(y) \tag{2}$$

where $p(x) = exp(-x^2/2)/\sqrt{2\pi}$.

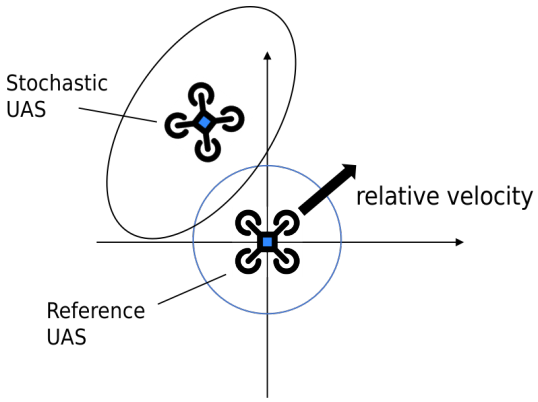

Fig. 7: Encounter geometry of stochastic and reference aircraft.

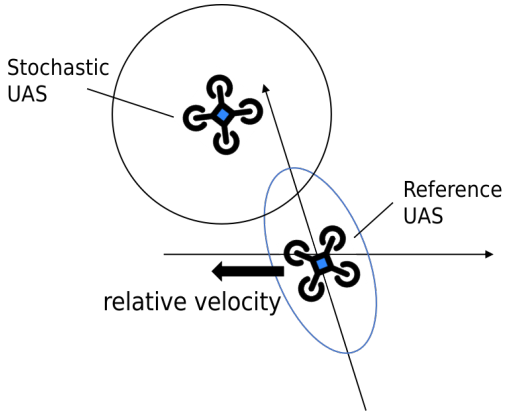

Fig. 8: Transformed encounter geometry where the combined error ellipse is transformed into a unit circle.

Rotate the relative velocity direction in parallel with x axis. Then the minimum and maximum values of Δy_c can be determined, and the conflict probability P_c can be simplified as:

$$\begin{aligned} P_c &= \int_{-\Delta y - \Delta y_c}^{-\Delta y + \Delta y_c} \int_{-\infty}^{\infty} p(x, y)\, dx\, dy \\ &= P(-\Delta y + \Delta y_c) - P(-\Delta y - \Delta y_c) \end{aligned} \tag{3}$$

where $\Delta y = y_S - y_R$ is the y coordinate of the two vehicle, and P is the cumulative normal probability function which is defined as:

$$P(z) \equiv \int_{-\infty}^{z} p(s)\, ds \tag{4}$$

where z is random variable. Thus, the problem of collision probability can be regarded as the difference between the two cumulative normal probability function.

The reader is directed to [26] for more details of this conflict probability estimation method. It should be noted that this paper is focused on horizontal conflict only.

Algorithm 1 FCFS pseudo algorithm.

While $f \in F$ **do**
  If f is *linear* flight **then**
    for (e,t), $(b_e,t) \in f_l$ **do** $\{e/b$: essential/buffer$\}$
      If (e,t) or (b_e,t) is blocked **then**
        Delay f_l for 1 time unit
        break
      else
        Insert (e,t) and (b_e,t) to $list_l$
    for (e,t) and $(b_e,t) \in list_l$ **do**
      Occupy $(e,t), (e, t \pm sep)$
      Occupy $(b_e,t), (b_e, t \pm sep)$

III. Conflict Resolution

This section presents two conflict resolution approaches, namely FCFS and optimisation, which incorporates the same probability-based conflict detection presented in Sec. II. The aim is to resolve any potential conflicts by means of delaying specific flights causing an estimated conflict probability over some threshold.

A. FCFS approach

Currently, the most commonly used approach for strategic conflict detection is based on the First-come, First-served (FCFS) principle. This approach examines potential conflicts between flight pairs, considering any level of overlap in both spatial and temporal aspects as a conflict. This approach is straightforward and fair in its detection of conflicts. The pseudo code for the FCFS algorithm is introduced in Algorithm 1. The fundamental of this algorithm is to have a common airspace information to represent the occupancy status of the airspace volumes, where each waypoint in the trajectory and its corresponding buffer space will occupy the airspace volumes during its planned operation time. Once a group of volumes have been occupied by early-submitted flight plans, they will not be available for the other subsequently submitted flight plans until the former operation ended. Thus, the conflict flights need to be delayed in time steps to resolve the conflict.

Algorithm 2 Conflict probability based FCFS pseudo algorithm.

1: **While** $F_x\_OV_m\_F_y\_OV_n \in$ intersection list **do**
2: F_x, F_y, OV_m, OV_n
3: **If** $t^s_{OV_m} < t^e_{OV_n} + t_{sep}$ and $t^s_{OV_n} - t_{sep} < t^e_{OV_m}$ **then**
4: $t_{delta} = |t^s_{OV_m} - t^s_{OV_n}|$
5: $OV^P \leftarrow min(t^s_{OV_m}, t^s_{OV_n})$
6: $OV^F \leftarrow max(t^s_{OV_m}, t^s_{OV_n})$
7: $OV^{UPD} \leftarrow OV^P + t_{delta} \cdot V_{OV^P} \cdot H_{OV^P}$
8: Calculate $prob(OV^{UPD}, V_{OV^P}, OV^F, V_{OV^F}, d_{sep})$
9: **If** $conflict\ probability \geqslant$ safety threshold **then**
10: $F^{lw} \leftarrow max(t^{sbm}_{F_x}, t^{sbm}_{F_y})$
11: Delay F^{lw} for 1 time unit
12: Update OV_m, OV_n
13: Go to Line 8
14: **else**
15: move to next intersection

The original FCFS algorithm is able to detect and resolve conflict in strategic phase. However, this approach is unable to identify insignificant intersections. To this end, this study revises the previous work and integrates conflict probability estimation into the process. As mentioned in Sec. II-D, a coarsely screening will be conducted before performing conflict probability estimation. The output of the coarse screening are the start and end time of the involved OV in each intersection $F_x\_OV_m\_F_y\_OV_n$. The conflict probability based FCFS approach will then checks the OV pairs sequentially based on the order in which the flights are submitted.

The pseudo code for conflict probability-based FCFS approach is presented in Algorithm 2. In comparison to the original FCFS approach, this probability based method retains the fundamental algorithmic idea while incorporating some enhancements. Firstly, instead of detecting and resolving conflict based on airspace representation form, intersected OV pairs are directly involved into the process. Secondly, the distance-based separation criteria is embedded in the probability estimation. Thirdly, the integrated conflict probability further examines the intersection, aiming to reduce the unnecessary delay. For intersected OVs that fail to meet both the spatial (as a result of conflict probability estimation) and temporal separation (as a result of time-based separation minima) criteria, delay action will be needed to resolve the conflict.

First, the time difference between the start time of the two intersected OVs will be calculated. Then, by comparing the start time of OVs, we can identify which OV will be first entered (previous) by the UAS and which is the later one (following). This is because the conflict probability is calculated based on the position of the UAS at a specific time. We use the OV entering time of the following UAS as the reference time, thus the position of the previous UAS at that time can be updated by the original position plus the product of multiplying the time difference with the speed and heading of the previous flight. Then, we calculate the conflict probability using coordinates of the starting and the end point of the two OV, the speed of the two UAS and the predefined safety separation, as introduced in Sec. II-E. If the probability is greater than the safety threshold, it means the risk of conflict is not acceptable and the flight with lower priority will be delayed by one time unit. The priority of the flight is determined by the flight submission time. Finally, we update the time of the delayed flight, and iterate to check conflict probability in a loop until the probability is less than the threshold or the two OVs meet the time-based separation requirement.

B. Optimisation Approach

In this section, we present the mathematical formulation of incorporating conflict probability in an optimisation model for strategic conflict resolution.

1) Decision variables: The model is formulated with mixed-integer linear programming and the corresponding decision variables are defined as follows:

$$x^j_{f,t} = \begin{cases} 1, & \text{if flight } f \text{ enters intersection } j \text{ by time } t \\ 0, & \text{otherwise} \end{cases}$$

It should be noted that the "by" time is used, while the "at" time can be derived from $(x^j_{f,t} - x^j_{f,t-1})$. In addition, if the entrance time to a specific OV (i.e., intersection j) for a flight has been determined, the exit time can be known, as the duration of OV is provided given the submitted flight plan.

2) Objective function: We consider an objective function minimising the overall delay for all flights, which can be computed by Eq. (5):

$$C_{delay} = \sum_{f \in F} \sum_{j \in J_f^{(1)}} \sum_{t \in T_f^{J_f^{(1)}}} (t - r_f^{J_f^{(1)}})(x^j_{f,t} - x^j_{f,t-1}), \quad (5)$$

where T^j_f is specific-defined subsets of time moments feasible for delay assignment. The initially scheduled take-off times are depicted by $r_f^{J_f^{(1)}}$. In the optimisation approach, each flight is assumed to be of the same priority, but the model will allow flight prioritisation by specifying their weighted costs of delay.

3) Flight operations constraints: The constraints are listed below, which can be grouped into flight operations, conflict probability, and the binary condition of the decision variables.

The following constraints are associated with the operational limits with regard to each individual flight.

$$x^j_{f,\underline{T}^j_f - 1} = 0,\ x^j_{f,\bar{T}^j_f} = 1 \quad \forall f \in F, \forall j \in J_f, \quad (6)$$

$$x^j_{f,t} - x^j_{f,t-1} \geqslant 0, \quad \forall f \in F, \forall j \in J_f, \forall t \in T^j_f, \quad (7)$$

$$x^{j'}_{f,t+\hat{t}^{jj'}_f} - x^j_{f,t} = 0, \quad \forall f \in F, \forall t \in T^j_f, j = J_f^{(i)}, \\ j' = J_f^{(i+1)} : \forall i \in [1, n_l), \quad (8)$$

Constraint (6) states that each flight should enter intersection j within a time window, where the upper and lower bound are described by $\bar{T}^j_f$ and $\underline{T}^j_f$ respectively. Constraint (7) enforces the continuity of the timeline by specifying the relationship of the flight entrance status between a certain time and its previous time unit. Constraint (8) stipulates that the controlled time between any two consecutive intersections (j, j') of a flight remain unchanged than initially scheduled.

4) Conflict probability constraints: The overall idea is to ensure that the conflict probability between any two flights (f, f'), at the same intersection j, to be lower or equal to a pre-defined threshold.

$$p(j, f, f', \Delta t)(x^j_{f,t} - x^j_{f,t-1} + x^j_{f',tp} - x^j_{f',tp-1} - 1) \leq p_s \\ \forall j \in J, \forall (f, f') \in F_j, f \neq f', \forall t \in T^j_f, \forall t' \in T^j_{f'}, \Delta t = t - t', \quad (9)$$

where $p(j, f, f', \Delta t)$ is pre-processed input to specify the conflict probability between any pair of flights (f, f') at their intersection j, with a varying time interval Δt that is equal to the difference between their OV entrance times (t, t') respectively. p_s is the maximum acceptable conflict probability.

To be specific, the pre-defined input $p(j, f, f', \Delta t)$ collects all the potential conflict OV pairs that are filtered by the coarsely screening and the time-based separation minima. Without knowing the delay assignment forehead, combinations of any possible delay allocations and their corresponding conflict probabilities for all potential conflict OVs will be store in $p(j, f, f', \Delta t)$. This ensures that all delay allocation scenarios are considered.

5) Decision variable conditions:

$$x^j_{f,t} \in \{0, 1\}, \forall f \in F, \forall j \in J_f, \forall t \in T^j_f. \quad (10)$$

Finally, Constraints (10) states the binary constraints and domains of the primary decision variables used in the model.

IV. Experimentation

This section presents numerical experiments with an illustrative scenario. We look into airspace that covers a 3-Dimensional space of 20*20 km^2 with a maximum altitude of 350 m, divided into 100*100*7 identical airspace volumes, leading to each volume of 200*200*50 m^3 size. Three case studies have been conducted, each then applying both conflict probability based FCFS and optimisation approaches, as well as their combined variant for an hybrid approach.

A. Scenario setup

The traffic sample includes 100 flights, which are 50 standard performing vehicles (SPVs) and 50 high performing vehicles (HPVs) through the 1 hour's overall duration, where the HPV and SPV are types of UAS used to perform specific operational tasks based on their performance capabilities, and their characterisation can be found in [27]. Types of airspace constraints based on real-world data are considered, including terrain obstacles, buildings that may influence operations, aeronautical and ground hazards, as introduced in Sec. II. The size of the OV (shape as rectangular) for each flight segment is set according to the performance of the UAS. The generated flight trajectories within the modelled 3D airspace environment are as shown in Fig. 9a.

Some experimental assumptions have been made: (1) the unit time step is set as 1 sec; (2) the speed of HPV and SPV are randomly set between 8-10 m/s and 3-5 m/s respectively; (3) The lateral distance between the boundary of the OV and the planned flight trajectory for HPV and SPV is set as 15 and 10 meters respectively; (4) a time-based separation minima of 15 sec and a distance-based separation minima (embedded in conflict probability estimation) of 35 meters are assumed; and (5) the safety threshold for the conflict probability is considered 99.99%.

In the experiments, Python has been used to develop the FCFS algorithm. For the optimisation approach, GAMS software suite has been used as the modelling tool and CPLEX as the solver. The experiments have been run on a 64 bit Intel®

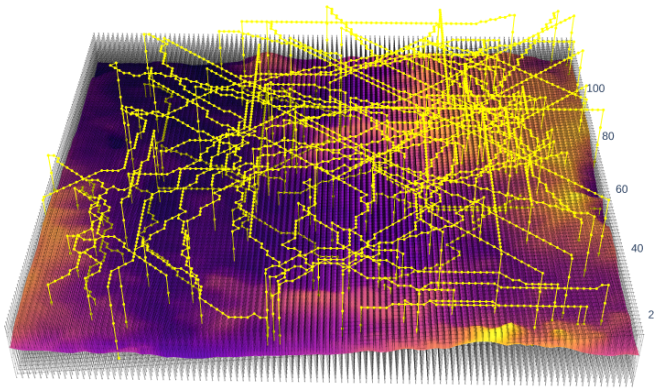

(a) Initial flight trajectories in airspace environment

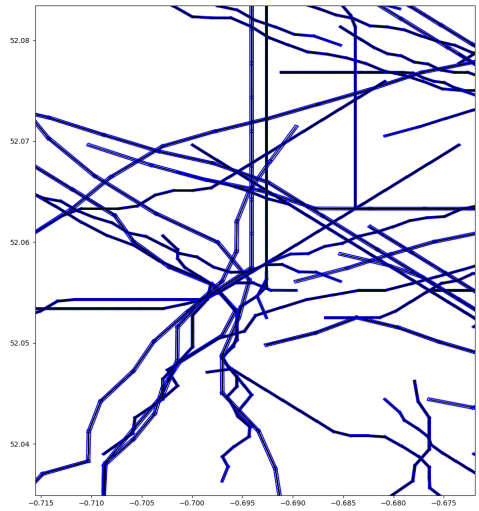

(b) Generated OVs for coarse conflict screening

Fig. 9: Illustrative scenario of flight trajectories and associated OVs used in the experimentation.

Core™ i5-9500 CPU @ 3.00GHz 6 Cores computer with 16 GB of RAM and Linux OS.

B. Case studies

The generated 100 flight plans are first sorted based on their submission order (which is defined arbitrarily). Depending on whether the FCFS/optimisation approach is selected to tackle a particular group of flights, three different case studies and their corresponding baseline cases are considered to gather a set of comparable solutions:

- **Case-1-O**: Full optimisation (original)
- **Case-1-P**: Full optimisation + conflict probability
- **Case-2-O**: Full FCFS (original)
- **Case-2-P**: Full FCFS + conflict probability
- **Case-3-O**: Hybrid (optimisation followed by FCFS)
- **Case-3-P**: Hybrid + conflict probability

To highlight the effectiveness of managing excessive delays, we conducted an additional experiment in each case that does not consider the probability integration. This experiment is referred to as the "original" case (denoted as '-O'). In contrast,

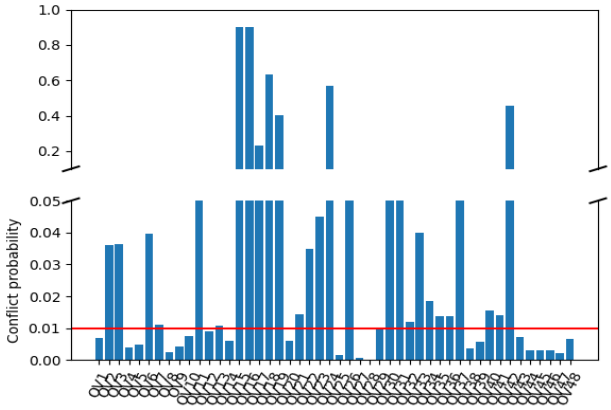

Fig. 10: Initial conflict probability for the identified OV pairs.

the case where probability is integrated is marked as '-P'. In Case-1 and Case-2, flight plans are exclusively processed using the optimisation and FCFS approaches. Case-3 employs a hybrid manner that combines two methods, in which the first half of the flight plans are processed with the optimisation approach, while the remaining half are dealt with by the FCFS approach. The rationale behind Case-3 is that some operations may be scheduled well in advance and can be handled in batch as a whole using the optimisation approach, while others are submitted shortly before takeoff and require individual processing using the FCFS approach. This approach closely resembles real-world operations, making it more representative than the first two cases.

C. Result comparison

After evaluating all submitted flight plans, we have identified that there are a total of 788 intersected OVs in the spatial perspective across all altitude levels. Additionally, 76 flights are found to be in conflict with other flights at their respective altitude levels. By applying a time-based separation minimum of 300 seconds, we identify 48 potential conflicted OVs after filtering. It is important to note that the setting of separation minima and the probability threshold significantly affect the number of conflicts observed. For instance, when the separation minimum is enlarged to 150 meters while maintaining a probability threshold of 99.99%, the number of conflicts decreases to 52. All the conflicts can be effectively resolved by either the FCFS or the optimisation approach. An overall comparison of the solutions derived from the above three case studies can be found in Table I, summarised in a few key indicators.

Regarding total delay, it is obvious to find that Case-1 required the least delay among the 3 cases, while Case-2 had the most. Regardless of whether probability is integrated or not, the total delay from Case-1 is less than half of that in Case-2. With conflict probability integrated, there are 197 and 666 time units of decrease in Case-1-P and Case-2-P respectively, which comes from the detection of non-

TABLE I: Result comparisons across the three cases of the study.

KPI	Case-1-O	Case-1-P	Case-2-O	Case-2-P	Case-3-O	Case-3-P
Total delay (sec)	473	276	1214	548	679	536
Delayed flights (a/c)	9	8	8	7	8	9
Average delay (sec)	53	35	152	78	85	60
Max delay (sec)	94	90	301	144	301	144
Total solution time (sec)	971	898	102	188	538	618

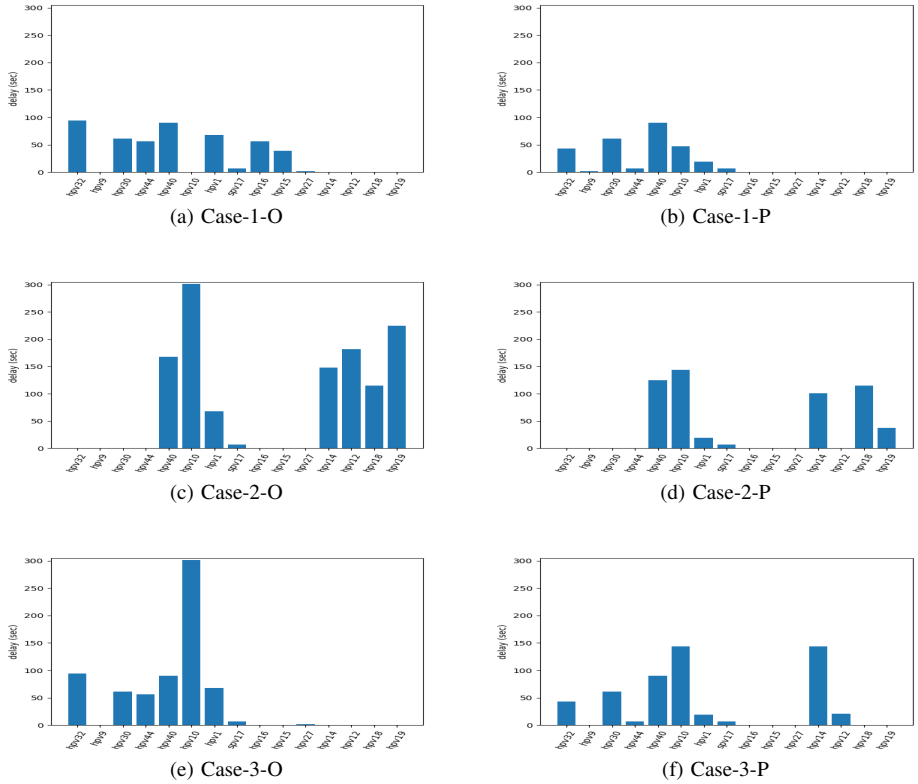

(a) Case-1-O (b) Case-1-P

(c) Case-2-O (d) Case-2-P

(e) Case-3-O (f) Case-3-P

Fig. 11: Distribution of delay allocation across all flights in each of the case studies.

significant intersection. The excessive delay (around 45%) is reduced by integrating the conflict probability.

Regarding the number of delayed flights, the values are quite similar among the three cases. As a result, the average delay across all three cases shows no significant variation. Specifically, Case-1 consistently maintains the lowest average delay, while Case-2 exhibits the highest delay. Case-3 falls in between, amalgamating characteristics from both of the other cases. It is worth to note that, after considering the probability of conflict, the average delays has been reduced approximately 40%. The impact of the algorithm is evident in the maximum delay, where the FCFS method results in delays three times longer than those produced by the optimization method. Additionally, in Case 3, the FCFS algorithm handles flights that incur significant delays, resulting in maximum delays identical to those observed in Case 2.

We further analysed the probability of potential conflict OVs after the conflict resolution process. It is not surprising to find that all the original cases had no remaining insignificant conflict OVs. As mentioned in Sec. IV-B, the conflict probability of all OVs in the original cases was considered to be 100%. Consequently, all potential OVs were treated as conflicts and delayed according to the respective rules. In the probability included cases, a few OV pairs were detected that did not meet the time-based separation. When analysing the maximum conflict probability among these remaining OVs, we could find that all probabilities were below the safe threshold. Therefore, even though these OV pairs did not meet the separation criteria, their intersection was considered insignificant due to the low probability of conflict. In Fig.10, the conflict probability of the 48 OV pairs is showed. The red line represents the safety threshold. As when some flights are delayed, new OV pairs may emerge that no longer meet the safety criteria. During the iterative screening process, these non-significant intersected OVs will be kept.

Upon examining the delay allocation for each flight, the results of flight conflict detection and resolution are presented in Fig. 11. The figure illustrates the outcomes obtained from

different cases and provides a comparison between the results when considering both conflict probability and without it. Based on the previous analysis, it was found that Case-1 resulted in the least total delay, while Case-2 had the highest total delay. When comparing the original case with the probability-based cases, it is evident that the application of the probability-based approach helped reduce certain delays.

V. Conclusions and further work

This paper introduced a conflict probability based strategic conflict resolution service aimed at UAS traffic management. The key finding is that, the airspace use could be further improved by allowing some overlapping between the Operational Volumes (OVs) as long as such overlapping does not yield an unacceptable conflict probability. To demonstrate the finding, this paper first presented the approach to generating OVs from smoothed flight trajectories in a realistic airspace environment. Then, a conflict detection method was elaborated that involves an initial coarse screening (based on purely temporal and spatial OVs overlapping) and a refined conflict probability estimation model. The detected conflict is then resolved by two proposed approaches, including FCFS and optimisation, fully incorporating the conflict detection outcome. A number of simulation experiments were conducted to prove the effectiveness of delay reduction as a result of conflict probability tolerance to a certain extent.

However, there are still many open issues that need to be addressed in future works. For instance, a key assumption made in this paper is that, both time-based and distance-based separation are essentially used, in which the former is for coarse conflict screening and the latter for conflict probability estimation. This may lead to an inconsistency of separation minima. Thus. further studies will be needed to better understand the relationship between the two separations. From the operational perspective, in addition to FCFS and batch optimisation, a more realistic scheme could be developed such as around the concept of Reasonable Time To Act (RTTA) proposed in U-space ConOps, to better handle the scenarios where flight plans are filed at different times in advance of activation. The conflict probability estimation model could be also extended from horizontal to vertical to meet the requirement of operating in 3D airspace environment.

Acknowledgement

This work was partially funded by the SESAR JU under grant agreement No 101017702, as part of the European Union's Horizon 2020 research and innovation programme: AMU-LED (Air Mobility Urban - Large Experimental Demonstrations). The opinions expressed herein reflect the authors view only. Under no circumstances shall the SESAR Joint Undertaking be responsible for any use that may be made of the information contained herein.

References

[1] P. Kopardekar, J. Rios, T. Prevot, M. Johnson, J. Jung, and J. E. Robinson, "Unmanned aircraft system traffic management (utm) concept of operations," in *AIAA Aviation and Aeronautics Forum (Aviation 2016)*, no. ARC-E-DAA-TN32838, 2016.

[2] Federal Aviation Administration, "Concept of operations," Tech. Rep. V2.0, 2022.

[3] CORUS-XUAM, "U-space concept of operations," SESAR JU, Tech. Rep. Edition 3.10, 2022.

[4] CORUS, "U-space concept of operations," SESAR JU, Tech. Rep. Edition 03.00.02, 2019.

[5] Y. Tang and Y. Xu, "Incorporating optimization in strategic conflict resolution for uas traffic management," *IEEE Transactions on Intelligent Transportation Systems*, pp. 1–13, 2023.

[6] E. L. Thompson, Y. Xu, and P. Wei, "A framework for operational volume generation for urban air mobility strategic deconfliction," in *2023 International Conference on Unmanned Aircraft Systems (ICUAS)*. IEEE, 2023, pp. 71–78.

[7] D. Sacharny, T. C. Henderson, M. Cline, B. Russon, and E. Guo, "FAA-NASA vs. Lane-Based Strategic Deconfliction," in *2020 IEEE International Conference on Multisensor Fusion and Integration for Intelligent Systems (MFI)*. IEEE, 2020, pp. 13–18.

[8] C. Chin, K. Gopalakrishnan, A. Evans, M. Egorov, and H. Balakrishnan, "Tradeoffs between efficiency and fairness in unmanned aircraft systems traffic management," in *Proceedings of the 9th International Conference on Research in Air Transportation (ICRAT)*, Castelldefels, Catalonia, Spain, 2020.

[9] F. Ho, R. Geraldes, A. Gonçalves, B. Rigault, B. Sportich, D. Kubo, M. Cavazza, and H. Prendinger, "Decentralized multi-agent path finding for uav traffic management," *IEEE Transactions on Intelligent Transportation Systems*, vol. 23, no. 2, pp. 997–1008, 2020.

[10] T. Dubot and A. Joulia, "Towards u-space conflict management services based on 4d protection bubbles," in *AIAA AVIATION 2021 FORUM*, 2021, p. 2347.

[11] M. Egorov, A. Evans, S. Campbell, S. Zanlongo, and T. Young, "Evaluation of UTM Strategic Deconfliction Through End-to-End Simulation," *14th USA/Europe ATM R&D Seminar*, 2021.

[12] M. Johnson and J. Larrow, "Uas traffic management conflict management model," 2020.

[13] A. standards, *Standard Specification for UAS Traffic Management (UTM) UAS Service Supplier (USS) Interoperability*. ASTM International, 2022.

[14] ICAO, "The longitudinal reich collision risk model," Tech. Rep. twentieth meeting, 2012.

[15] Y. Zou, H. Zhang, G. Zhong, H. Liu, and D. Feng, "Collision probability estimation for small unmanned aircraft systems," *Reliability Engineering & System Safety*, vol. 213, p. 107619, 2021.

[16] L. Yang and J. Kuchar, "Using intent information in probabilistic conflict analysis," in *Guidance, Navigation, and Control Conference and Exhibit*, 1998, p. 4237.

[17] S. Endoh, "Aircraft collision models," Ph.D. dissertation, Massachusetts Institute of Technology, 1982.

[18] BUBBLES project, "Algorithm for analysing the collision risk," Tech. Rep. D4.1, 2021.

[19] ——, "Guidelines to implement separation minima and methods," Tech. Rep. D4.2, 2021.

[20] A. angel. (2023) The home if unified traffic management. [Online]. Available: https://www.altitudeangel.com/

[21] Y. Tang, Y. Xu, and G. Inalhan, "An integrated approach for on-demand dynamic capacity management service in u-space," *IEEE Transactions on Aerospace and Electronic Systems*, pp. 1–16, 2022.

[22] M. Elbanhawi, M. Simic, and R. N. Jazar, "Continuous path smoothing for car-like robots using b-spline curves," *Journal of Intelligent & Robotic Systems*, vol. 80, pp. 23–56, 2015.

[23] D. Nakamura and W. Royce, "Operational benefits of performance-based navigation," *Boeing Aero Quarterly, Quarter*, vol. 2, pp. p13–21, 2008.

[24] R. Geister, L. Limmer, M. Rippl, and T. Dautermann, "Total system error performance of drones for an unmanned pbn concept," in *2018 Integrated Communications, Navigation, Surveillance Conference (ICNS)*. IEEE, 2018, pp. 2D4–1.

[25] C. J. Wang, E. M. Ng, and K. H. Low, "Investigation and modeling of flight technical error (fte) associated with uas operating with and without pilot guidance," *IEEE Transactions on Vehicular Technology*, vol. 70, no. 12, pp. 12 389–12 401, 2021.

[26] R. A. Paielli and H. Erzberger, "Conflict probability estimation for free flight," *Journal of Guidance, Control, and Dynamics*, vol. 20, no. 3, pp. 588–596, 1997.

[27] AMU-LED, "D2.2.010 high level conops - initial," SESAR JU, Tech. Rep. Edition 00.01.00, 2021.

2023-11-10

Conflict probability based strategic conflict resolution for UAS traffic management

Tang, Yiwen

IEEE

Tang Y, Xu Y, Inalhan G. (2023) Conflict probability based strategic conflict resolution for UAS traffic management. In 2023 IEEE/AIAA 42nd Digital Avionics Systems Conference (DASC), 1-5- October 2023, Barcelona, Spain

https://doi.org/10.1109/DASC58513.2023.10311236